physics

MDPI

Communication

Modeling the Magnetic Field of the Inner Corona in a Radially Expanding Solar Wind

Andrey G. Tlatov * and Ivan Berezin

Kislovodsk Mountain Astronomical Station of the Pulkovo Observatory, Gagarina Str. 100, 357700 Kislovodsk, Russia

* Correspondence: tlatov@mail.ru

Abstract: The magnetic field in the interplanetary medium is formed by the action of magnetic field sources on the photosphere of the Sun and currents in the expanding atmosphere of the Sun and the solar wind. In turn, the high-speed plasma flow changes the configuration of the magnetic field lines. The problem of determining the parameters of the magnetic field near the Sun is thus a three-dimensional problem of the interaction of the magnetic field and the plasma of the solar wind. We present analytical expressions for calculating the total magnetic field vector $\vec{B}(r, \theta, \phi)$ (in spherical coordinates) for a radially expanding solar wind flow of finite conductivity. The parameters of the solar wind are given in the form of a dimensionless magnetic Reynolds number given as an arbitrary function of the radius, r: $R_m = r\sigma\mu v = \xi(r)$, where σ, μ, and v denote, respectively, the conductivity, magnetic permeability, and velocity of the solar wind. The solution for the magnetic field components is obtained in the form of a decomposition in spherical functions and a radial part depending on the distance from the Sun. Examples of calculations of the configuration of magnetic fields and structures of the solar corona for the solar eclipse of 21 August 2017 are given.

Keywords: solar wind; solar corona; solar magnetic field model

Citation: Tlatov, A.G.; Berezin, I. Modeling the Magnetic Field of the Inner Corona in a Radially Expanding Solar Wind. *Physics* **2023**, *5*, 161–167. https://doi.org/10.3390/physics5010012

Received: 29 November 2022
Revised: 6 January 2023
Accepted: 9 January 2023
Published: 29 January 2023

1. Introduction

The magnetic field in the solar corona and the interplanetary medium is formed by the action of the photospheric magnetic field and electric currents in the solar wind. The interaction of the magnetic field and plasma in the near-solar space leads to the formation of structures in the corona, observed, for example, in white light during eclipses. In turn, the high-speed plasma flow changes the configuration of the magnetic field lines. The problem of determining the parameters of the magnetic field near the Sun, taking into account the expanding solar wind, generally remains unsolved. Simplifying assumptions are usually used to solve the problem.

In recent years, significant progress has been made in constructing realistic three-dimensional global magneto-hydrodynamic (MHD) models [1,2]. Such models are necessary for a self-consistent description of the interaction of the magnetic field with the plasma in the solar atmosphere. These models allow comparison of the calculated coronal structure with observations and provide simulations of solar wind parameters in the heliosphere; see, e.g., [1,3]. On the other hand, MHD models require external boundary conditions (e.g., plasma densities or temperatures), and here the problem of solution ambiguity remains relevant.

To solve the problem, simplifying assumptions are usually applied. Early calculations of the magnetic field in the solar corona neglected the presence of a conductive medium, reducing the problem to a search for the scalar potential near a charged sphere [4]. However, at distances $r > 1.5 - 2R_\odot$, where $R_\odot$ is the radius of the Sun, this approximation turns out to be poorly applicable, since it does not satisfactorily describe the topology of the magnetic field, as well as the law of decreasing magnitude of the magnetic field with distance. In the

potential approximation, it is proportional to $1/r^3$. Actually, the observed magnetic field decreases with distance according to the law, $\sim 1/r^{2.13}$ [5].

To eliminate the disagreement, a source surface is introduced, on which the potential turns to zero [4]. The approximation of the source surface is to simulate the effect of solar wind outflow, which distorts the magnetic field from a non-current configuration above approximately $\sim 2.5 R_\odot$ The application of the source surface is only a geometric approach in a potential approximation and does not take into account the real parameter α of the solar wind.

Another approach is the approximation, in which the magnetic field is drawn by an expanding solar corona with infinite conductivity [6,7]. This approximation inadequately describes the behavior of the magnetic field at small distances from the Sun and leads to the understanding that the magnetic field in this model decreases in proportion to $1/r^2$. The magnetic field lines in this approximation appear radial even in the inner corona of the Sun. Thus, the real picture corresponds to the conditions of finite plasma conductivity or non-potential models.

The potential field model gives a rough approximation for large-scale solar magnetic structures and is suitable when a small electric current is present. Later, a linear simulation of the force-free field was developed with a constant parameter α, which is the proportionality between the electric current and the magnetic field [8]. However, observations show that α is usually inconstant for the magnetic field of the Sun [9]. A more realistic model is a model of a force-free field with a variable parameter α. Such a nonlinear force-free field (NLFFF) is used to calculate the three-dimensional magnetic field in the corona (see [8] and references therein).

An alternative to global MHD modeling that requires significant computational resources is the magneto-friction (MF) method [8,10,11]. In this method, instead of solving the full MHD momentum equation, the velocity, v, is approximated by the magnetofriction form introduced in Ref. [10]. In Ref. [12], a development of the MF model, which uses a given solar wind profile, is proposed.

At the same time, analytical solutions for non-potential configurations of the magnetic field in the Sun's low corona remain relevant. One type of such solution is magnetohydrostatic approximations [13]. Other models consider magnetic field propagation in a radially expanding solar wind flow of finite conductivity. In Ref. [14], solutions for determining the magnetic field components, $B_r,\ B_\theta,\ B_\phi$, in spherical coordinates $(r,\ \theta,\ \phi)$, is given for the case when the conductivity, σ, and velocity, v, both depend on the radius, r. The solution for B_r was found from the solution of a second-order differential equation by reducing it to a first-order equation and, further, by decomposition over a large parameter by the WKB (Wentzel–Kramers–Brillouin) approximation. The components $B_\theta,\ B_\phi$ were found from B_r.

In this paper, we will look for solutions for the magnetic field near the Sun, taking into account the radially expanding solar wind with finite electrical conductivity.

2. Some Explicit Solutions

This Section provides a solution for determining the total magnetic field vector, $\vec{B}$, for a radially expanding solar wind flow of finite conductivity, $\sigma(r)$, homogeneous in θ, ϕ [15]. Bogdan and Low [13] proposed a method for representing the magnetic field for the static radially stratified atmosphere of the Sun through the scalar functions, Ψ and Φ:

$$\vec{B} = \Psi\left(r, \frac{\partial \Phi}{\partial r}\right)\vec{e}_r + \frac{1}{r}\frac{\partial \Phi}{\partial \theta}\vec{e}_\theta + \frac{1}{r\sin\theta}\frac{\partial \Phi}{\partial \phi}\vec{e}_\phi, \tag{1}$$

where $\vec{e}_r$, $\vec{e}_\theta$, and $\vec{e}_\phi$ are the unit vectors.

Similar to that in Ref. [13], we assume that the current, J, is directed perpendicular to gravity. In the case here, we consider that the quasipermanent solar wind propagates radially: $v = v_r$, and the current J is formed by the interaction of the radially expanding

wind and the magnetic field. Then, from Equation (1) and the equation, $\nabla \times B = \mu J$, one gets the equation for the horizontal current:

$$\mu \vec{J} = \frac{1}{r \sin\theta} \frac{\partial\left(\Psi - \frac{\partial \Phi}{\partial r}\right)}{\partial \phi} \vec{e}_\theta - \frac{1}{r} \frac{\partial\left(\Psi - \frac{\partial \Phi}{\partial r}\right)}{\partial \theta} \vec{e}_\phi, \tag{2}$$

where μ is the magnetic permeability.

From $\mathrm{div}\vec{B} = 0$, it follows:

$$\frac{\partial(r^2\Psi)}{\partial r} + \frac{1}{\sin\theta}\left(\frac{\partial \sin\theta \frac{\partial \Phi}{\partial \theta}}{\partial \theta} + \frac{1}{\sin\theta}\frac{\partial^2 \Phi}{\partial \varphi^2}\right) = 0. \tag{3}$$

This equation can be linearized if

$$\Psi\left(r, \frac{\partial \Phi}{\partial r}\right)\vec{e}_r = \eta(r)\frac{\partial \Phi}{\partial r}\vec{e}_r, \tag{4}$$

where $\eta(r)$ is some function of r. Substituting this expression into Equation (3), one obtains:

$$\frac{\partial(r^2\eta \frac{\partial \Phi}{\partial r})}{\partial r} + \frac{1}{\sin\theta}\left(\frac{\partial \sin\theta \frac{\partial \Phi}{\partial \theta}}{\partial \theta} + \frac{1}{\sin\theta}\frac{\partial^2 \Phi}{\partial \varphi^2}\right) = 0. \tag{5}$$

The basic solution of this equation can be represented as a decomposition:

$$\Phi(r,\ \theta,\ \phi) = \sum_{n=0}^{\infty} \sum_{m=-n}^{n} A_{nm} \Phi_n(r) Y_n^m(\theta, \varphi), \tag{6}$$

where A_{nm} are constant coefficients. Φ_n—linearly independent solutions of the equation:

$$\frac{\partial\left(r^2\eta \frac{\partial \Phi_n}{\partial r}\right)}{\partial r} - n(n+1)\Phi_n = 0, \tag{7}$$

and the function $Y_n^m(\theta,\ \phi)$ is expressed in terms of the attached Legendre polynomials, $P_n^m(\theta,\ \phi)$:

$$Y_n^m = (-1)^m \left[\frac{(2n+1)}{4\pi}\frac{(n-m)!}{(n+m)!}\right]^{1/2} P_n^m(\cos\theta)\exp(im\varphi). \tag{8}$$

Electrical current, J, can be expressed through generalized Ohm's law, $\vec{J} = \sigma(\vec{E} + \vec{v} \times \vec{B})$, where σ is the specific electrical conductivity. Since in the stationary case, $\nabla \times \vec{E} = -\partial\vec{B}/\partial t = 0$, we assume that the electric field $\vec{E} = 0$. Then, the current J is expressed through the speed v of the solar wind and the magnetic field:

$$\vec{J} = \sigma(\vec{v} \times \vec{B}) = v\sigma(B_\theta \vec{e}_\phi - B_\phi \vec{e}_\theta). \tag{9}$$

Converting Equation (9), while taking into account Equation (1), one ontains:

$$\vec{J} = -\frac{\sigma v}{r \sin\theta}\sum_n \sum_m^n \Phi_n \frac{\partial Y_n^m}{\partial \varphi}\vec{e}_\theta + \frac{\sigma v}{r}\sum_n \sum_m^n \Phi_n \frac{\partial Y_n^m}{\partial \theta}\vec{e}_\varphi. \tag{10}$$

On the other hand, from Equations (2), (4), and (6), one obtains:

$$\begin{aligned}\mu\vec{J} &= \frac{1}{r}\sin\theta\frac{\partial}{\partial\phi}\left(\sum_n\sum_m^n \eta\frac{d\Phi_n}{dr}Y_n^m - \sum_n\sum_m^n \frac{d\Phi_n}{dr}Y_n^m\right)\vec{e}_\theta \\ &- \frac{1}{r}\frac{\partial}{\partial\theta}\left(\sum_n\sum_m^n \eta\frac{d\Phi_n}{dr}Y_n^m - \sum_n\sum_m^n \frac{d\Phi_n}{dr}Y_n^m\right)\vec{e}_\phi \\ &= \sum_n\sum_m^n \frac{(\eta-1)}{r\sin\theta}\frac{d\Phi_n}{dr}\frac{\partial Y_n^m}{\partial\phi}\vec{e}_\theta - \sum_n\sum_m^n \frac{(\eta-1)}{r}\frac{d\Phi_n}{dr}\frac{\partial Y_n^m}{\partial\theta}\vec{e}_\phi.\end{aligned} \tag{11}$$

Comparing Equations (10) and (11), one finds:

$$J_\theta = -\frac{\sigma v}{r\sin\theta}\sum_n\sum_m^n \Phi_n\frac{\partial Y_n^m}{\partial\phi} = \sum_n\sum_m^n \frac{(\eta-1)}{r\mu\sin\theta}\Phi_n^{'}\frac{\partial Y_n^m}{\partial\varphi}, \tag{12}$$

$$J_\phi = \frac{\sigma v}{r}\sum_n\sum_m^n \Phi_n\frac{\partial Y_n^m}{\partial\theta} = -\sum_n\sum_m^n \frac{(\eta-1)}{r\mu}\Phi_n^{'}\frac{\partial Y_n^m}{\partial\theta}, \tag{13}$$

where the prime denotes the derivative with respect to r. Using the orthogonality of Legendre polynomials, one obtains from the equations for currents (12), (13):

$$\sigma\mu\, v\Phi_n = (1-\eta)\Phi_n^{'}, \tag{14}$$

or

$$\eta = 1 - \sigma\mu\, v\Phi_n/\Phi_n^{'}. \tag{15}$$

Taking into account Equation (15), the second-order differential Equation (7) is transformed into a first-order equation:

$$\frac{d}{dr}(r^2\eta\Phi_n^{'}) - n(n+1)\Phi_n = \frac{d}{dr}\left(\frac{r^2\eta\sigma\mu\, v\Phi_n}{1-\eta}\right) - n(n+1)\Phi_n = 0, \tag{16}$$

Denoting $y_n = r^2\eta\sigma\mu\, v\Phi_n/(1-\eta)$, Equation (16) can be rewritten as

$$y_n' = \frac{(1-\eta)}{r^2\eta\sigma\mu\, v\Phi}n(n+1)y_n = f(r)n(n+1)y_n, \tag{17}$$

where $f(r) = (1-\eta)/(r^2\eta\sigma\mu\, v)$. This equation can be solved by separating variables:

$$\frac{dy_n}{y_n} = f(r)n(n+1)dr, \tag{18}$$

having a general form of the solution:

$$\ln(y_n) = \int_{R=R_0}^{r} f(r)n(n+1)dr. \tag{19}$$

From Equation (19), one obtains a general expression for Φ_n:

$$\Phi_n = A\frac{(1-\eta)}{r^2\eta\sigma\mu\theta v}\exp\left(\int_{R=R_0}^{r} f(r)n(n+1)dr\right), \tag{20}$$

where A is a constant. For a complete solution (6), A_{nm} can be determined from the signal on the photosphere, $F(\theta,\ \phi)$:

$$A_{nm} = \int F(\theta,\ \phi)Y_n^m(\theta,\ \phi)d\Omega, \tag{21}$$

where Ω is the solid angle.

Consider the special case when $|\eta| \gg 1$. Then one can neglect 1 in Equations (14) and (15):

$$\Phi_n = (1-\eta)\Phi_n^{'}/(\sigma\mu\, v) \simeq -\eta\Phi_n^{'}/(\sigma\mu\, v), \tag{22}$$

and then $f(r)$ is independent of η:

$$f(r) = (1-\eta)/(r^2\eta\sigma\mu\, v) \simeq -1/(r^2\sigma\mu\, v). \tag{23}$$

The dimensionless quantity, $r\sigma\mu v$, is equal to the magnetic Reynolds number and in the current consideration is a function of distance: $R_\mathrm{m} = r\sigma\mu v = f(r)$. Then, at $|\eta| \gg 1$, the solutions for $\vec{B}$ can be written in the form:

$$B_r = \sum_n \sum_m^n \frac{A_{nm}}{r^2} \exp\left(\int_{R=R_0}^r -\frac{n(n+1)}{rR_\mathrm{m}} dr\right) Y_n^m, \tag{24}$$

$$B_\theta = \sum_n \sum_m^n \frac{-A_{nm}}{r^2 R_\mathrm{m}} \exp\left(\int_{R=R_0}^r -\frac{n(n+1)}{rR_\mathrm{m}} dr\right) \frac{\partial Y_n^m}{\partial\theta}, \tag{25}$$

$$B_\phi = \sum_n \sum_m^n \frac{-A_{nm}}{r^2 \sin\theta R_\mathrm{m}} \exp\left(\int_{R=R_0}^r -\frac{n(n+1)}{rR_\mathrm{m}} dr\right) \frac{\partial Y_n^m}{\partial\phi}. \tag{26}$$

3. Simulation of the Coronal Magnetic Field at the Time of the Solar Eclipse on 21 August 2017

Let us consider examples for calculating the configuration of the magnetic field in the corona. To set the magnetic field, synoptic maps of the Sun's magnetic fields are used. The Kislovodsk Mountain Astronomical Station (KMAS) performs daily measurements of the magnetic fields of the Sun [16,17]. For modeling, let us use synoptic maps with a resolution of 720 × 360. For calculations, the procedure of filling the poles and polar correction is performed. The polar correction, i.e., the conversion of the LOS (line of sight) component into the radial $B_r(r = R_\odot)$, is carried out by dividing by the cosine of latitude. For calculations according to the scheme (24)–(26), it is necessary to set the function $R_\mathrm{m}(r) = \xi(r)$. The calculations were carried out with the approximation of the R_m function with the power dependence, $R_\mathrm{m}(r) = R_\mathrm{m}^0 r^\alpha$. When integrating, one obtains:

$$\int_{R=R_0}^r \frac{1}{rR_\mathrm{m}} dr = -\frac{1}{R_\mathrm{m}^0 r^\alpha \alpha}. \tag{27}$$

The values of the R_m number, which has the meaning of the magnetic Reynolds number, lie in the range from 0.1 to 10. For values of $R_\mathrm{m} > 10$, the calculation gives only direct radial rays, and for $R_\mathrm{m} < 0.5$ there is a case of a potential magnetic field.

The calculation procedure consisted of several stages: (i) preparation of a synoptic map of magnetic fields; (ii) decomposition of the magnetic field into spherical harmonics; (iii) restoration of the magnetic field vector in the solar corona and obtaining a picture of ray structures.

Figure 1 shows the results of modeling the shape of the corona at the time of the solar eclipse of 21.08.2017. For comparison, calculations for potential approximation of the potential-field source-surface model (PFSS) and non-potential approximation (NP) using Equations (24)–(26) are also presented. For the NP the parameters of the radial function were chosen as $R_\mathrm{m}^0 = 1.5$, $\alpha = 2.5$. Such values were chosen for the best fit of the configuration of the field lines to the observations. It can be noted that the configurations of the field lines are similar. The regions of closed magnetic field lines correspond to the of helmet-shaped rays of the observed solar corona [18]. In the polar regions, one can find the open configurations of magnetic fields, corresponding to of polar plumes. For the selected NP parameters at low altitudes, the field lines rise to lower heights than in the potential PFSS calculation. Despite the absence of source surface conditions, in NP calculations, the magnetic field lines are also close to the radial direction.

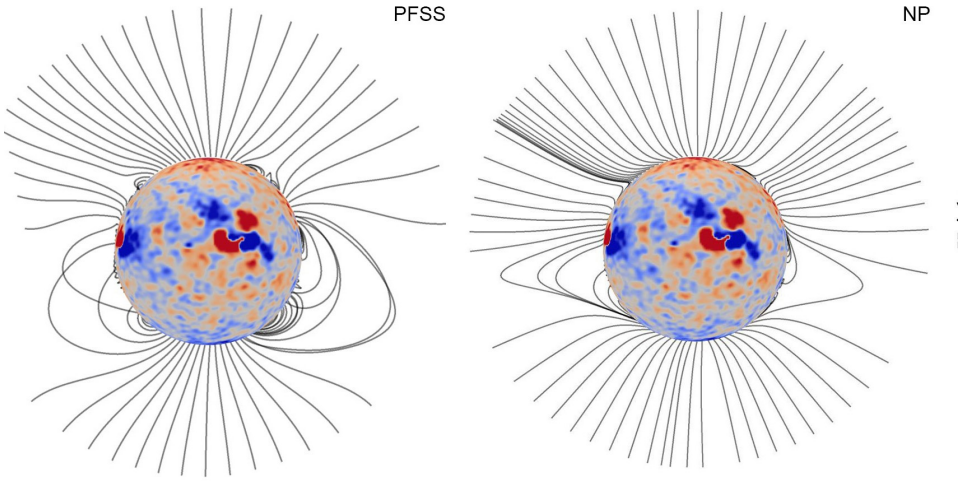

Figure 1. Configuration of magnetic field lines for 21.08.2017 for potential approximation (PFSS) and for non-potential approximation (NP). See text for details.

4. Conclusions

Global magnetic fields can be modeled using MHD models. At the same time, the problem of forming boundary conditions for MHD at the lower boundary remains urgent. As a rule, the potential PFSS approximation and the Wang-Sheeley-Arge (WSA) model [19] for calculating solar wind parameters are used for this.

The solution considered here for a non-potential case can help in solving this problem. Setting the radial function for $R_{\mathrm{m}}(r) = \xi(r)$ gives more freedom and can take into account the differences in the formation of the coronal magnetic field at different phases of the activity cycle. The presented solution for the required computing resources is comparable to calculations using PFSS methods. Just like in PFSS, spherical functions are used to describe the magnetic field. This makes it possible to use this solution to estimate the parameters of the solar wind in the WSA scheme.

Thus, the presented non-potential method of calculating the magnetic field can be used to reconstruct the topology of the solar corona, used in estimating the speed of the solar wind and used to set boundary conditions for MHD models.

Author Contributions: Conceptualization, A.G.T.; methodology, A.G.T.; software, I.B. and A.G.T.; validation, I.B.; formal analysis, A.G.T.; investigation, A.G.T. and I.B; resources, A.G.T.; data curation, I.B.; writing—original draft preparation, A.G.T.; writing—review and editing, A.G.T. and I.B.; visualization, I.B.; supervision, A.G.T.; project administration, A.G.T.; funding acquisition, A.G.T. All authors have read and agreed to the published version of the manuscript.

Funding: This research was funded by Russian Science Foundation (project No. 23-22-00165).

Data Availability Statement: The data presented in this study are available in Ref. [17].

Acknowledgments: The authors thank the anonymous reviewer for useful comments and inaccuracies found in the original text of the manuscript.

Conflicts of Interest: The authors declare no conflict of interest.

References

1. Riley, P.; Lionello, R.; Linker, J.A.; Mikic, Z.; Luhmann, J.; Wijaya, J. Global MHD modeling of the solar corona and inner heliosphere for the whole heliosphere interval. *Sol. Phys.* **2011** *274*, 361–377. [CrossRef]
2. Feng, X.; Yang, L.; Xiang, C.; Jiang, C.; Ma, X.; Wu, S.T.; Zhong, D.; Zhou, Y. Validation of the 3D AMR SIP-CESE solar wind model for four Carrington rotations. *Sol. Phys.* **2012**, *279*, 207–229. [CrossRef]
3. Tóth, G.; van der Holst, B.; Sokolov, I.V.; de Zeeuw, D.L.; Gombosi, T.I.; Fang, F.; Manchester, W.B.; Meng, X.; Najib, D.; Powell, K.G.; et al. Adaptive numerical algorithms in space weather modeling. *J. Comput. Phys.* **2012**, *231*, 870–903. [CrossRef]
4. Altschuler, M.D.; Newkirk, G., Jr. Magnetic Fields and the structure of the solar corona. I: Methods of calculating coronal fields. *Sol. Phys.* **1969**, *9*, 131–149. [CrossRef]

5. Behannon, K.W. Mariner 10 interplanetary magnetic field results. In *Physics of Solar Planetary Environments: Proceedings of the International Symposium on Solar-Terrestrial Physics, Boulder, CO, USA, 7–18 June 1976*; Williams, D.J., Ed.; American Geophysical Union: Washington, DC, USA, 1976; Volume 1, pp. 332–345. [CrossRef]
6. Parker, E.N. Dynamics of the interplanetary gas and magnetic fields. *Astrophys. J.* **1958**, *120*, 664–676. [CrossRef]
7. Pneuman, G.W.; Kopp, R.A. Gas-magnetic field interactions in the solar corona. *Sol. Phys.* **1971**, *18*, 258–270. [CrossRef]
8. Mackay, D.H.; Yeates, A.R. The Sun's global photospheric and coronal magnetic fields: Observations and models. *Liv. Rev. Sol. Phys.* **2012**, *9*, 6. [CrossRef]
9. Schrijver, C.J.; DeRosa, M.L.; Metcalf, T.R.; Liu, Y.; McTiernan, J.; Régnier, S.; Valori, G.; Wheatl, M.S.; Wiegelmann, T. Nonlinear force-free modeling of coronal magnetic fields. Part I: A quantitative comparison of method. *Sol. Phys.* **2006**, *235*, 161–190. [CrossRef]
10. Yang, W.H.; Sturrock, P.A.; Antiochos, S.K. Force-free magnetic fields: The magneto-frictional method. *Astrophys. J.* **1986**, *309*, 383–391. [CrossRef]
11. Mackay, D.H.; Upton, L.A. A comparison of global magnetofrictional simulations of the 2015 March 20 solar eclipse. *Astrophys. J.* **2022**, *939*, 9. [CrossRef]
12. Rice, O.E.K.; Yeates, A.R. Global coronal equilibria with solar wind outflow. *Astrophys. J.* **2021**, *923*, 57. [CrossRef]
13. Bogdan, T.J.; Low, B.C. The three-dimensional structure of magnetostatic atmospheres. II. Modeling the large-scale corona. *Astrophys. J.* **1986**, *306*, 271–283. [CrossRef]
14. Chertkov, A.D. *Solar Wind and Internal Structure of the Sun*; Nauka Publishers: Moscow, Russia, 1985. (In Russian)
15. Tlatov, A.G. Modeling of a large-scale magnetic field in a radially expanding corona with finite conductivity. *Bull. Sol. Data [Bull. Solnech. Dannye]* **1993**, *8*, 76–80. (In Russian)
16. Tlatov, A.G.; Dormidontov, D.V.; Kirpichev, R.V.; Pashchenko, M.P.; Shramko, A.D.; Peshcherov, V.S.; Grigoryev, V.M.; Demidov, M.L.; Svidskii, P.M. Study of some characteristics of large-scale solar magnetic fields during the global field polarity reversal according to observations at the telescope-magnetograph Kislovodsk Observatory. *Geomagn. Aeron.* **2015**, *55*, 969–975. [CrossRef]
17. Kislovodsk Mountain Astronomical Station. Available online: http://solarstation.ru (accessed on 3 January 2023)
18. Mikić, Z.; Downs, C.; Linker, J.A.; Caplan, R.M.; Mackay, D.H.; Upton, L.A.; Riley, P.; Lionello, R.; Török, T.; Titov, V.S.; et al. Predicting the corona for the 21 August 2017 total solar eclipse. *Nat. Astron.* **2018**, *2*, 913–921. [CrossRef]
19. Arge, C.N.; Pizzo, V.J. Improvement in the prediction of solar wind conditions using near-real time solar magnetic field updates. *J. Geophys. Res. Space Phys.* **2000**, *105*, 10465–10479. [CrossRef]